



**HAL**  
open science

## Direct synthesis of pure brannerite $UTi_2O_6$

Adel Mesbah, Stephanie Szenknect, Nicolas Clavier, Hantao Lin, Fabien Baron, Daniel Beaufort, Yann Batonneau, Julien Mercadier, Aurélien Eglinger, Marion Turuani, et al.

► **To cite this version:**

Adel Mesbah, Stephanie Szenknect, Nicolas Clavier, Hantao Lin, Fabien Baron, et al.. Direct synthesis of pure brannerite  $UTi_2O_6$ . *Journal of Nuclear Materials*, 2019, 515, pp.401-406. 10.1016/j.jnucmat.2019.01.003 . hal-01979146

**HAL Id: hal-01979146**

**<https://hal.science/hal-01979146>**

Submitted on 13 Nov 2020

**HAL** is a multi-disciplinary open access archive for the deposit and dissemination of scientific research documents, whether they are published or not. The documents may come from teaching and research institutions in France or abroad, or from public or private research centers.

L'archive ouverte pluridisciplinaire **HAL**, est destinée au dépôt et à la diffusion de documents scientifiques de niveau recherche, publiés ou non, émanant des établissements d'enseignement et de recherche français ou étrangers, des laboratoires publics ou privés.

# Direct synthesis of pure brannerite $UTi_2O_6$

Adel Mesbah,<sup>1,\*</sup> Stéphanie Szenknect,<sup>1</sup> Nicolas Clavier,<sup>1</sup> Hantao Lin,<sup>1</sup> Fabien Baron,<sup>2</sup> Daniel Beaufort,<sup>3</sup> Yann Batonneau,<sup>3</sup> Julien Mercadier,<sup>4</sup> Aurélien Eglinger,<sup>4</sup> Marion Turuani,<sup>5</sup> Philippe Goncalves,<sup>5</sup> Flavien Choulet,<sup>5</sup> Virginie Chapon,<sup>6</sup> Anne-Magali Seydoux-Guillaume,<sup>7</sup> Maurice Pagel,<sup>8</sup> Nicolas Dacheux.<sup>1</sup>

1- ICSM, CEA, CNRS, ENSCM, Univ Montpellier, Site de Marcoule - Bât. 426, BP 17171, 30207 Bagnols-sur-Cèze, France

2 – Université de Nantes - CNRS Laboratoire de Planétologie et Géodynamique, 2 rue de la Houssinière, 44322 Nantes, France

3- Université de Poitiers, CNRS UMR 7285 IC2MP, HydrASA Bât. B35, rue Michel Brunet, 86022 Poitiers Cedex, France

4- Université de Lorraine, CNRS, CREGU, GeoRessources Laboratory, B.P. 70239, F-54506 Vandœuvre-lès-Nancy, France

5- Chrono-Environnement, UMR 6249, CNRS-Université de Bourgogne Franche-Comté, Besançon, France

6- CEA, CNRS, Aix-Marseille Université, UMR 7265 Biologie Végétale et Microbiologie Environnementales, Laboratoire des Interactions Protéine Métal, Saint-Paul-lez-Durance, France

7- Université de Lyon, UJM-Saint-Etienne, CNRS, UCA, IRD, LMV UMR 6524, Saint-Etienne, France

8- GEOPS, Univ Paris Sud, CNRS, Université Paris-Saclay, Rue du Belvédère, Bât. 504, Orsay F-91405, France

## Abstract:

A new method based on the precipitation of uranium(IV) and titanium(IV) hydroxide precursors was developed to prepare pure brannerite  $UTi_2O_6$  samples. In fact, U(IV) dissolved in HCl (6 mol.L<sup>-1</sup>) was mixed to Ti (IV) alkoxyde before a basification step with an excess of  $NH_4OH$  to obtain a highly reactive powder of a nanometric  $(U,Ti)(OH)_4$ . The obtained powder was then dried under vacuum, pressed into pellets and finally fired at 1300°C. The refined unit cell parameters of  $UTi_2O_6$  led to  $a = 9.8113(2) \text{ \AA}$ ,  $b = 3.7681(1) \text{ \AA}$ ,  $c = 6.9232(1) \text{ \AA}$ ,  $\beta = 118.94(1)^\circ$  and  $V = 223.9(1) \text{ \AA}^3$ . This method led to the formation of pure brannerite in contrast to previous reported protocols, which showed the formation of impurities such as  $UO_2$  and  $TiO_2$ .

**Keywords:** brannerite, uranium titanate, uranium hydroxide

Corresponding author

E-mail address: [Adel.mesbah@cea.fr](mailto:Adel.mesbah@cea.fr) (A. MESBAH)

## Introduction

In uranium deposits under reducing environments, uraninite ( $\text{UO}_2$ ) and coffinite ( $\text{USiO}_4$ ) are the main uranium (IV) ore minerals. Brannerite ( $\text{UTi}_2\text{O}_6$ ) represents a significant third resource of tetravalent uranium in many deposits. However, it is strongly refractory to dissolution in current milling processes and requires a heating step in the chemical processes which significantly increases the cost of uranium extraction from the ore. Brannerite is presently reported to occur in several geological environments such as Elliot Lake (Ontario, Canada) [1, 2], Mount Isa (Australie) [3, 4], Kirovograd (Ukraine), Crocker Well (Australia) [5], Domes Region (Zambia) [6] and also in some uraniferous deposits in the Witwatersrand area (South Africa) [7]. Moreover, brannerite is also detected in exploited uranium mines in Australia such as Ranger or Olympic Dam [4]. In nature, brannerite is usually found as an amorphous form subsequently to self-radiation damage (metamictization) [8, 9]. The annealing of the crystal network requires a thermal treatment at 1000 °C. Additionally, brannerite is also considered as a minor phase entering the composition of several Synroc families, which have been developed in the field of immobilization of actinides from nuclear wastes [10].

Brannerite is reported to be strongly refractory to dissolution [5]. The uranium recovery often requires the use of aggressive conditions such as  $0.5 \text{ mol L}^{-1} \text{ H}_2\text{SO}_4$  above 75 °C. One explanation of this property arises from the presence of titanium in the structure, which can lead to the formation of titanium hydroxide then titanium oxide acting as a passivation layer on the surface of the mineral when saturation conditions are reached in the dissolution media. Therefore, different dissolution studies developed on synthetic and natural brannerite suggested a strong benefit coming from the use of oxidative conditions associated to the presence of  $\text{Fe}^{3+}$  species.

From a structural point of view, brannerite crystallizes in a monoclinic system with the  $\text{C2/m}$  space group. The structure consists of infinite layers formed by  $\text{TiO}_6$  octahedra separated by  $\text{UO}_6$  octahedra down the  $c$  axis as viewed in **Figure 1**.

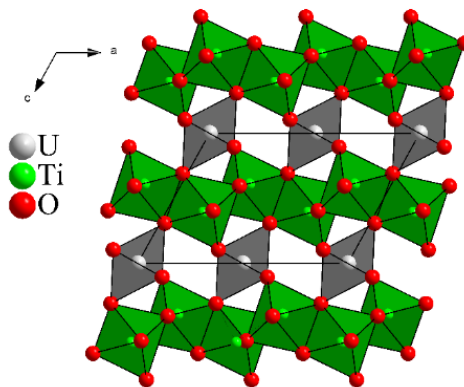


**Figure 1.** Representation of the crystal structure of  $UTi_2O_6$  down the b axis

According to literature, synthetic brannerite samples were obtained by different routes. As instance, it was obtained by firing a mixture of uranium and titanium dioxides at high temperature. Indeed, Helean et al. [11] obtained brannerite samples by heating the mixtures ( $UO_2+TiO_2$ ) at  $1200^\circ C$  for 300 h under  $CO - 5\% / CO_2 - 95\%$  atmosphere. Other chemical routes involving the precipitation of low-temperature precursors were also developed. First, we can cite the case of the “Alkoxide/nitrate” route [12, 13] and the “Acetate” route developed by Hussein et al [14] then used by Charalambous et al. [15]. All these chemistry routes require extended mechanical grinding step during the fabrication process, which are usually considered as a heavy step when handling radioactive materials. In addition, this grinding process cannot guaranty the homogenization in terms of cationic distribution (U, Ti), which could result in the formation of  $UO_2$  and/or  $TiO_2$  as secondary phases. Moreover, the latter techniques use U(VI) based reactants as starting precursors. Additionally, the working atmosphere under which the thermal treatment is performed was not always specified in the literature, except by Vance et al. [13] who mentioned the need to perform the experiments under low oxygen content ( $pO_2 < 10^{-5}$  atm). Consequently, the oxidation state of uranium in the synthesized brannerite is not always well established. Collela *et al.*[16] performed an exhaustive study on the valence state of uranium in natural and synthetic brannerite samples using a combination of techniques. They showed that even in synthetic samples prepared by the alkoxide-nitrate processing route, the average valence state of uranium was 4.3 due to the presence of a significant amounts of  $U^{5+}$  and  $U^{6+}$  in the structure and reached 4.4 to 4.7 in natural samples.

Considering that the presence of secondary phases (mainly  $UO_2$ ) resulting from the method of synthesis and the oxidation state of uranium in brannerite have a potential role in the alteration mechanisms and in the release rates upon exposure to aqueous fluids, there is a need

to develop new ways of syntheses avoiding the precipitation of actinides as less refractory secondary phases and allowing the control of the oxidation state of uranium. Ultimately, such a synthetic sample could be used as a reference material either to study the mechanisms of dissolution of ores containing brannerite, to identify brannerite in ores using spectroscopic techniques or to determine the valence states of uranium in natural and substituted brannerites. With the aim, this paper is devoted to the preparation and characterization of pure brannerite samples following three synthesis protocols reported in the literature namely alkoxide/nitrate method (1), acetate method (2) and dry chemistry route from  $\text{UO}_2 + \text{TiO}_2$  mixtures (3). Several drawbacks associated to the three chemistry routes were then solved by the development of a new method based on the precipitation of a uranium (IV) and titanium (IV) hydroxide mixture (4).

## Experimental section

### Synthesis.

The reactants during the synthesis, i.e.  $\text{NH}_4\text{OH}$  ( $\geq 99\%$ ), titanium alkoxyde ( $\geq 97\%$ ),  $\text{TiO}(\text{SO}_4)\cdot n\text{H}_2\text{O}$  (29%  $\text{TiO}_2$  basis), and  $\text{H}_2\text{C}_2\text{O}_4\cdot 2\text{H}_2\text{O}$  ( $\geq 99\%$ ) were of analytical grade and were purchased from Sigma Aldrich, uranyl acetate was home made. The uranium source was kindly provided by CETAMA France. Uranium (IV) chloride was obtained by dissolving uranium metal chips in  $6 \text{ mol L}^{-1}$   $\text{HCl}$ . For U(VI) supply, a concentrated uranyl nitrate solution was used. The final concentration of each solution was determined by ICP-AES. In order to synthesize brannerite, the four different chemistry routes listed below were considered.

1. “Acetate route” [14, 15]: this method consisted in simultaneous dissolution of uranyl acetate (2.33 mmol) and titanyl sulphate dihydrate (4.66 mmol) in 1 L of a solution containing 120 g oxalic acid . The mixture was dried in air at  $200 \text{ }^\circ\text{C}$  then heated at  $600 \text{ }^\circ\text{C}$  under  $\text{Ar}/\text{H}_2$  for 5 h in order to eliminate the organic part and other residues and with the goal to obtain oxides ( $\text{UO}_2$  and  $\text{TiO}_2$ ). The obtained powder was ground, pressed into pellets then thermally heated at  $1300 \text{ }^\circ\text{C}$  for 96 h.
2. “Alkoxide/nitrate” route [12, 13]: this method consisted in the mixing of solutions containing uranyl nitrate (1.16 mmol) and titanium alkoxyde (2.32 mmol) in 100 mL of water. The solution was dried in air at  $200 \text{ }^\circ\text{C}$ , heated in air at  $750 \text{ }^\circ\text{C}$  for 1 h leading to the elimination of nitrates and residues coming from the organic part

leading also to the formation of oxides ( $U_3O_8 + TiO_2$ ). The obtained powder was then wet milled for 16 h, pressed into pellets then fired at 1300 °C for 14 h.

3. “Dry chemistry route”. For this method, a mixture containing powdered  $UO_2$  and  $TiO_2$  was mechanically ground during 16 h at room temperature, pressed into pellets then thermally heated at 1300 °C for 96 h.
4. “Hydroxide precipitation route”. The hydroxide method was adapted from the synthesis protocol developed by Martinez *et al* [17], which was initially used for the synthesis of uranium dioxide. In this frame, three experiments were carried out. The first one consisted in mixing solutions of U (IV) chloride ( $2.33 \text{ mmol L}^{-1}$ ) and of Ti-alkoxyde solution ( $4.66 \text{ mmol L}^{-1}$ ) with 17 mL of deionized water. Then, an excess of  $NH_4OH$  (46.6 mmol) was added leading to the formation of a uranium-titanium bearing hydroxide brownish gel. After 30 min of stirring, the mixture was washed twice by centrifugation in water and once in ethanol. For the second test, a Ti excess of 3 mol.% of titanium was added in the mixture. The third set consisted in the addition of titanium alkoxyde in the solution after the precipitation of  $U(OH)_4 \cdot nH_2O$ .

For all the conditions, the final powder dispersed in ethanol was dried under vacuum at 40 °C leading to de-agglomerated powder having a large specific surface area (larger than  $100 \text{ m}^2 \cdot \text{g}^{-1}$ ) [17]. The powder was then compacted into a green pellet then placed in a furnace at 1300 °C for 96 h under argon atmosphere.

Whatever the method followed in this work, the thermal treatment at 1300°C under Ar atmosphere was conducted on pellets in order to favor the diffusion between the elements with the goal to obtain pure brannerite.

### **Powder X-Ray Diffraction (PXRD)**

The obtained samples were firstly ground using an agate mortar, then the resulting powders were analyzed by PXRD using Bruker D8 Advance diffractometer equipped with copper radiation ( $Cu \text{ K}\alpha_{1,2}$ ,  $\lambda = 1.54184 \text{ \AA}$ ) and using the reflection geometry. The powders were placed in special confined sample holders in order to avoid any radioactive contamination. The PXRD patterns were collected in the angular range of  $5 \leq 2\theta \leq 100^\circ$  with a total counting time of about 3 h. In addition, PXRD pattern of pure silicon standard was collected in similar conditions in order to extract the instrumental function. The collected data were refined by the

Rietveld method with the use of the Fullprof\_Suite package [18]. During the refinement, different profile and structure parameters were allowed to vary. Moreover, an anisotropic size model was added for each phase to simulate the microstructural effect.

## **NIR**

The visible and near-infrared spectrum of the synthetic brannerite was acquired in the 350–2500 nm range using the field ASD spectrometer TerraSpec<sup>®</sup>. The spectrometer was equipped by one Si detector (350-1000 nm range) and two InGaAs detectors (1000-2500 nm) having a spectral resolution of 4 nm and 8 nm, respectively. The acquisition was conducted using a contact probe including a white light source (halogen bulb). The presented spectrum of the synthetic brannerite resulted from an average of 35 scans.

## **Raman spectroscopy**

Raman spectra were recorded by the means of a Horiba - Jobin Yvon Aramis apparatus equipped with an edge filter and using a Nd:YAG laser (532 nm). In order to avoid any laser-induced degradation of the compound, the power was turned down to about 5 mW by the means of an optical filter. The laser beam was then focused on a small fraction of powder simply deposited on a glass lamella using an Olympus BX 41 microscope. A  $\times 50$  objective with a numerical aperture of 0.8, resulting in a spot size of about  $1 \mu\text{m}^2$  was used. The scattered Raman light was collected in a  $180^\circ$  backscattering geometry and dispersed by a grating of 1800 grooves/mm after having passed a  $150 \mu\text{m}$  entrance slit, resulting in a spectral resolution lower than  $1 \text{ cm}^{-1}$ . For each spectrum, a dwell time of 15 s was considered with an average of 4 scans. Before analysis, the apparatus was calibrated with a silicon wafer, using the first-order Si line at  $520.7 \text{ cm}^{-1}$  with an accuracy lower than  $1 \text{ cm}^{-1}$ .

The band component analysis was carried out by the means of the Jandel Peakfit software, using pseudo-Voigt functions (Gaussian-Lorentzian ratio systematically higher than 0.7) with the minimum number of components. Correlation coefficient  $R^2$  greater than 0.994 was obtained.

## Results and discussion

Whatever the protocol considered in routes (1), (2), (3), brannerite ( $\text{UTi}_2\text{O}_6$ ) was always obtained as the major phase. PXRD patterns corresponding to the powders obtained following the three first protocols are reported in **Figure 2**. However, the prepared samples were polyphase since the presence of uranium dioxide ( $\text{UO}_2$ ) was always observed as secondary phase. No sign of unreacted titanium (e.g. present as  $\text{TiO}_2$ ) was evidenced. For each sample, the weight contents of each phase (brannerite and  $\text{UO}_2$ ) and the unit cell parameters were determined by Rietveld refinement (**Table 1**). The uranium dioxide content was clearly dependent on the synthesis route; varying from 1 wt.% (dry chemistry route) up to 25 wt.% (acetate route).

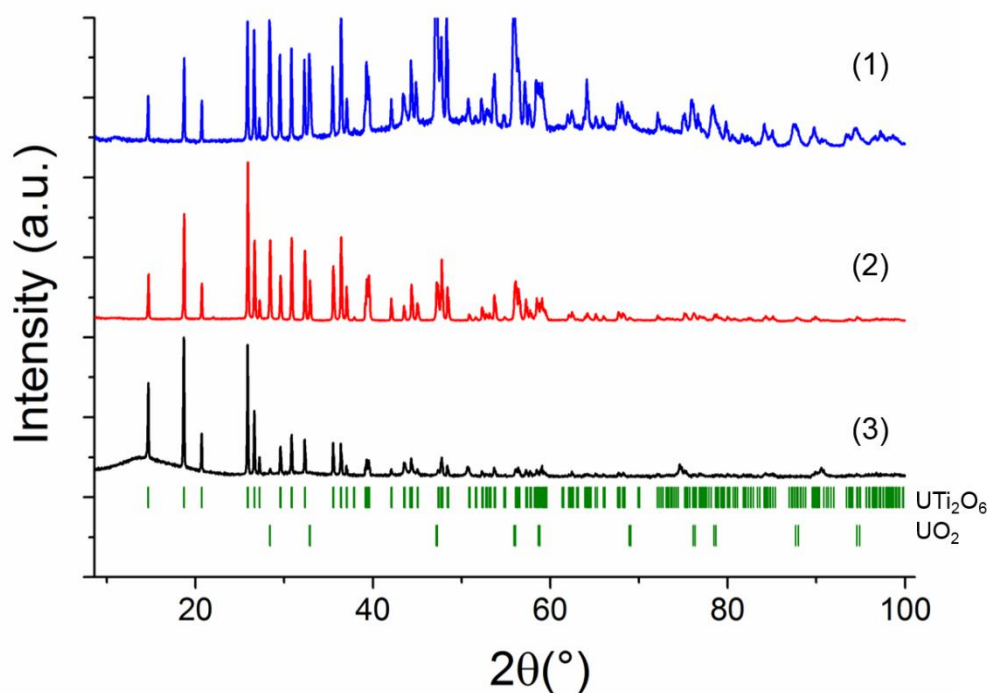


**Figure 2.** PXRD patterns obtained for brannerite samples prepared by “acetate route” (1), “alkoxide/nitrate route” (2) and dry chemistry route (3)

**Table 1.** Refined unit cell parameters and weight contents of  $\text{UTi}_2\text{O}_6$  and  $\text{UO}_2$  (expressed in wt.%). Obtained for the samples prepared by “acetate route” (1), “alkoxide/nitrate route” (2) and dry chemistry route (3).

	$a$ (Å)	$b$ (Å)	$c$ (Å)	$\beta$ (°)	$V$ (Å <sup>3</sup> )	$V_{\text{UO}_2}$ (Å <sup>3</sup> )	wt.% $\text{UTi}_2\text{O}_6$	wt.% $\text{UO}_2$
# 1	9.8144(3)	3.7672(2)	6.9193(3)	118.87(1)	224.02(1)	162.56(1)	75 ± 2	25 ± 2
# 2	9.8176(2)	3.7606(1)	6.9050(1)	118.90(1)	223.17(1)	161.55(1)	87 ± 1	13 ± 1
# 3	9.8171(2)	3.7591(1)	6.9017(2)	118.94(1)	222.88(1)	161.79(4)	99 ± 1	1 ± 1
[19]	9.8123(15)	3.7697(6)	6.9253(9)	118.957(6)	224.14			

The results obtained from the Rietveld refinement confirmed the formation of brannerite (as the main phase) and  $\text{UO}_2$  in the prepared powder. The methods based on the precipitation of a low temperature precursor (i.e. acetate and alkoxide/nitrate routes) showed the presence of large amounts of  $\text{UO}_2$  compared to that obtained by dry chemistry route (i.e. mixture of  $\text{UO}_2$  and  $\text{TiO}_2$ ). This is certainly due to some difficulties in the weighing of the appropriate amounts of titanium (either under the form of  $\text{TiOSO}_4 \cdot n\text{H}_2\text{O}$  and/or  $\text{Ti}[\text{OCH}(\text{CH}_3)_2]_4$ ) caused by variable hydration ratios and hygroscopic character of the samples that induce non-stoichiometric mixtures of U and Ti with a lack of Ti. Moreover, the successive steps of evaporation and calcination could influence the homogeneity of the starting mixtures of precursors. Although dry-chemistry route allows precise weighing of the starting powders, it did not lead to a single-phase material maybe due to lack of reactivity of the oxides powders and slow diffusion of both titanium and uranium in the starting mixtures.

In addition, the refined unit cell parameters were compared to those reported in the literature. In the case of the application of the “acetate method” (1), the unit cell volume of the brannerite was found to be 224.02(1) Å<sup>3</sup>, which is close to the value reported by J. Szymanski et al, [19] (i.e. 224.14 Å<sup>3</sup>). On the contrary, the unit cell volumes obtained for “alkoxide/nitrate” and “dry chemistry” routes were found to be slightly lower. This could be explained by the presence of small amounts of U(VI) within the structure. In the case of the “acetate route”, the calcination of the precursor was performed under  $\text{Ar}/\text{H}_2$ , which led to the reduction of uranium into its tetravalent form. In the case of the “alkoxide/nitrate” and “dry chemistry” routes, uranium was either introduced in higher oxidation state than 4+ because of the milling step leading to the formation of  $\text{U}_3\text{O}_8$ . Then after,  $\text{U}_3\text{O}_8$  decomposed under low oxygen content into  $\text{UO}_{2+x}$  above 1000 °C. Therefore, regardless the followed method, the obtained brannerite was not pure and contained various amounts of  $\text{UO}_2$  as by-product. Moreover, there are some

practical drawbacks associated with these protocols such as the evaporation of the initial solution at 200 °C, a milling step for more than 12 h involving a radioactive element, which could increase the risk of contamination.

Since the samples prepared by the three first methods did not result to a single phase, a new method based on the precipitation of uranium and titanium hydroxide precursor followed by its direct heating at 1300 °C was developed without any prior heating or grinding step. The PXRD patterns obtained for the three types of “hydroxide precipitation” methods are gathered in [Figure 3](#).

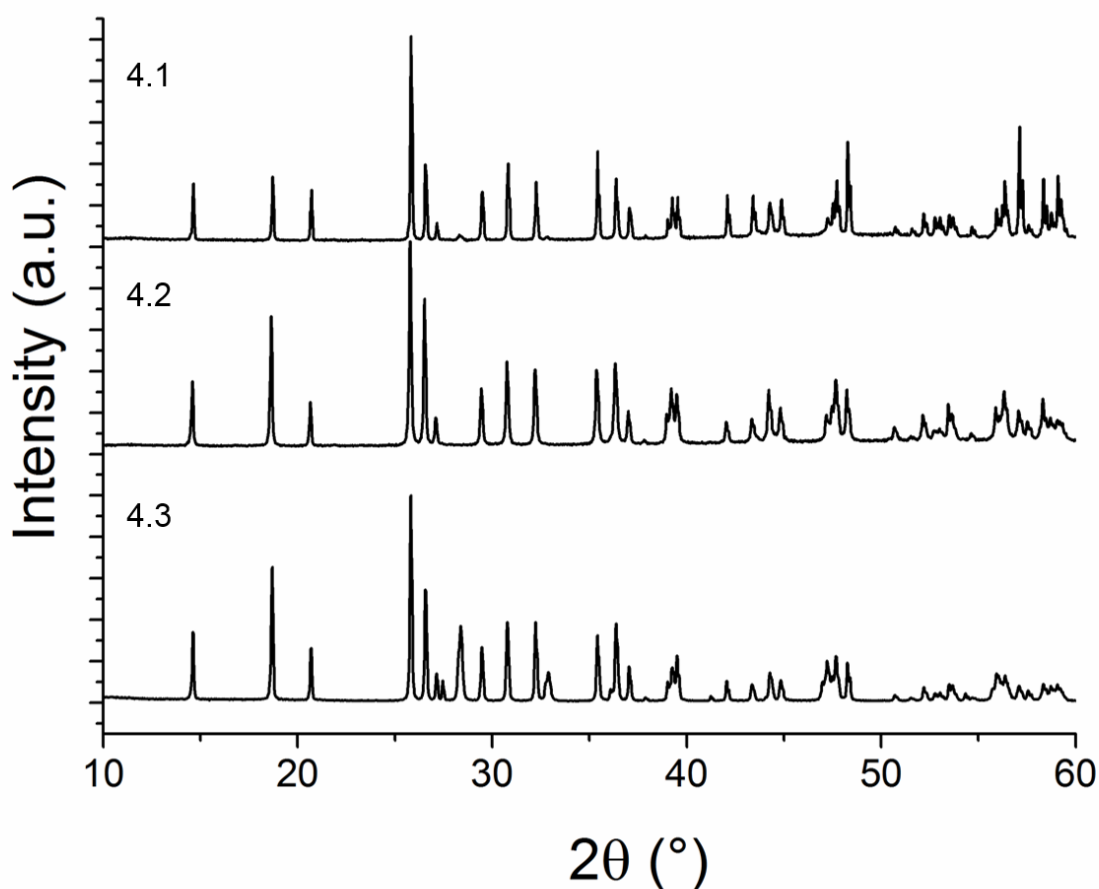


**Figure 3.** PXRD patterns collected for the samples prepared by the three varieties of “hydroxide precipitation” route (4). U(IV) + Ti-alkoxyde (4.1), with addition of 3 mol.% excess of titanium (4.2), with addition of Ti-alkoxyde after basification (4.3).

The analysis of the PXRD patterns reported in [Figure 3](#) showed that whatever the “hydroxide precipitation” route considered, brannerite (UTi<sub>2</sub>O<sub>6</sub>) was always obtained as the main phase. However, when using the first or the third variety, the formation of impurities (i.e.

UO<sub>2</sub> and TiO<sub>2</sub>) was detected. The weight contents of secondary phases as well as the unit cell parameters refined by the Rietveld method are reported in **Table 2**.

**Table 2.** Refined unit cell parameters for the synthesized UTi<sub>2</sub>O<sub>6</sub> and weight amount (wt %) found for each phase.

	<i>a</i> (Å)	<i>b</i> (Å)	<i>c</i> (Å)	$\beta$ (°)	<i>V</i> (Å <sup>3</sup> )	wt.% UTi <sub>2</sub> O <sub>6</sub>	wt.% UO <sub>2</sub>	wt.% TiO <sub>2</sub>
# 4.1	9.8115(1)	3.7693(1)	6.9255(1)	118.94(1)	224.1(1)	91.5 ± 8	8.5 ± 2	---
# 4.2	9.8113(2)	3.7681(1)	6.9232(1)	118.94(1)	223.9(1)	100	---	---
# 4.3	9.8098(1)	3.7686(1)	6.9227(1)	118.87(1)	224.1(1)	78.1 ± 8	12.6 ± 3	9.3 ± 6

The refined unit cell parameters of the three brannerite samples prepared using the hydroxide routes are in good agreement with those reported in the literature (224.14 Å<sup>3</sup>) [19]. In fact the use of U(IV) based reactants as starting precursors certainly prevents the oxidation of uranium in the brannerite structure. Moreover, from the synthesis (4.1) the weighing of the stoichiometric amounts led to the formation of UO<sub>2</sub> considered as an impurity. This could be explained by the underestimation of the introduced titanium amount into the reaction because of the hydrolysis and polycondensation of Ti, or by a possible insertion of titanium into the uranium site. Therefore, in order to avoid any lack of titanium in the starting mixture, a slight excess of titanium (i.e. 3 mol.%) was added during the preparation of the precursor. From the results reported in **Figure 3** and in **Table 2**, the synthesis led to pure brannerite with no need of additional grinding and/or re-heating step. On the contrary, when using the third “hydroxide precipitation” variety, the uranium dioxide content in the final sample was significantly higher than that obtained for the two other varieties. This could result from a degradation of the homogeneity of the mixture of the precursors due to the separated precipitation of uranium and titanium. In this latter case, the benefit coming from the use of the “hydroxide precipitation” route was clearly counterbalanced. This benefit relies on the preparation of a homogeneous and intimate mixture of nanometric hydroxide precursors. The large surface area developed between Ti and U(IV) hydroxide particles associated to the nanometric size of Ti and U(IV)-rich domains give the mixture its high reactivity.

### Near-Infrared spectroscopy

The visible and near-infrared spectrum of the synthetic brannerite includes several weak absorption bands in the 350-1000 nm wavelength range (**Figure 4**). This result is in contradiction with the studies of Finnie et al. [20] and Vance et al. [13], where the authors did not observe any spectral features within this wavelength range for synthetic brannerite, which was prepared by alkoxide/nitrate route. However, the position and the relative intensity of bands observed in the present spectrum of the synthetic brannerite prepared by the new hydroxide route (4.2) match very well with the spectra of  $U^{4+}$ -doped thorutite ( $Th_{1-x}U_xTi_2O_6$ ) presented by Finnie et al. [20]. The observed absorption bands correspond to the electronic transitions of  $U^{4+}$  ions in the brannerite structure. No evidence of  $U^{5+}$ , characterized by an intense and sharp absorption band around 1450 nm as described by Vance et al. [13], Finnie et al. [20] and Zhang et al. [21] was observed in the spectrum of synthetic brannerite.

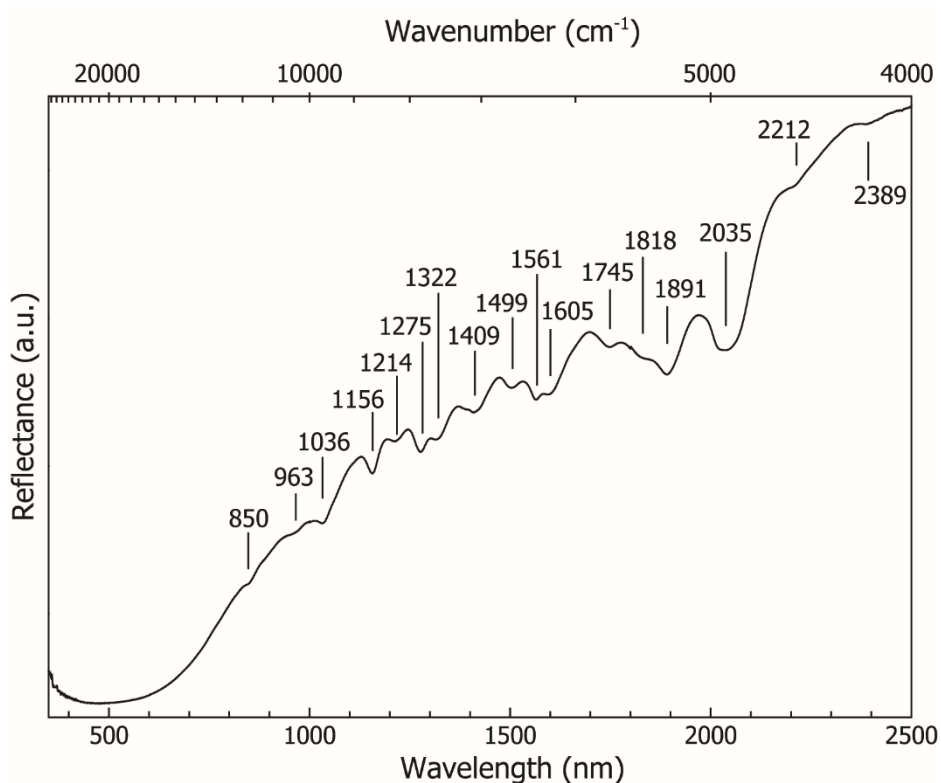


**Figure 4.** Visible / Near-IR spectrum of the synthetic brannerite ( $UTi_2O_6$ ) prepared by the hydroxide route (4.2). The position of the spectral features are expressed in nm.

### Raman spectroscopy

The Raman spectra collected for the various synthetic samples of  $UTi_2O_6$  were all found to present similar features. An example is provided in **Figure 5**. As the structure of brannerite is composed by  $UO_6$  and  $TiO_6$  polyhedra, the modes that can be observed mainly correspond to

the vibrations of oxygen atoms. Indeed, the factor group analysis provided by Zhang et al. [22] leads to:

$$\Gamma = 8A_g + 4B_g + 5A_u + 10B_u \quad (3)$$

Among these modes,  $2A_g + B_g + 2A_u + 4B_u$  accounts for external translation motions, while the remaining  $6A_g + 3B_g$ , and  $3A_u + 6B_u$ , are Raman and infrared active, respectively. All the bands observed in the 100-1000  $\text{cm}^{-1}$  domain were found to be in good agreement with those already reported for synthetic samples of brannerite [22], as well as for Ce- [23] and Th-bearing [24] counterparts. Particularly, the stretching vibrations of the (Ti-O-Ti) moiety lead to the most intense band at 760  $\text{cm}^{-1}$  for the antisymmetric mode, and to a weak band at 488  $\text{cm}^{-1}$  for  $\nu_s(\text{Ti-O-Ti})$ . Based on an analogy with isostructural vanadates [25], the two bands located at 571 and 632  $\text{cm}^{-1}$  were then assigned to the  $\text{Ti}_2\text{O}_2$  bridges corresponding to the edges shared between two  $\text{TiO}_6$  octahedra. The assignment of the three bands observed at 272, 331 and 374  $\text{cm}^{-1}$  appeared to be more complicated but was sometimes described as the result of the combination of (Ti-O-Ti) bending with stretching modes of  $\text{UO}_6$  polyhedra [23]. Finally, the vibration modes occurring below 200  $\text{cm}^{-1}$  are correlated to lattice external modes.

Compared to natural samples, the most obvious difference is the absence of vibration bands correlated with the stretching vibrations of the uranyl entity ( $\text{UO}_2^{2+}$ ) [26], which confirms that uranium is fully incorporated in the tetravalent oxidation state in the synthetic brannerite. Also, one must note that no band associated with the  $\text{TiO}_2$  by-product (such as that pointed out by Zhang et al. around 435  $\text{cm}^{-1}$  [22]) was observed. On this basis, the Raman spectroscopy argues for the formation of a pure and single-phase  $\text{UTi}_2\text{O}_6$  sample after firing at 1300 °C of the precursor obtained by “hydroxide precipitation” route (4.2).

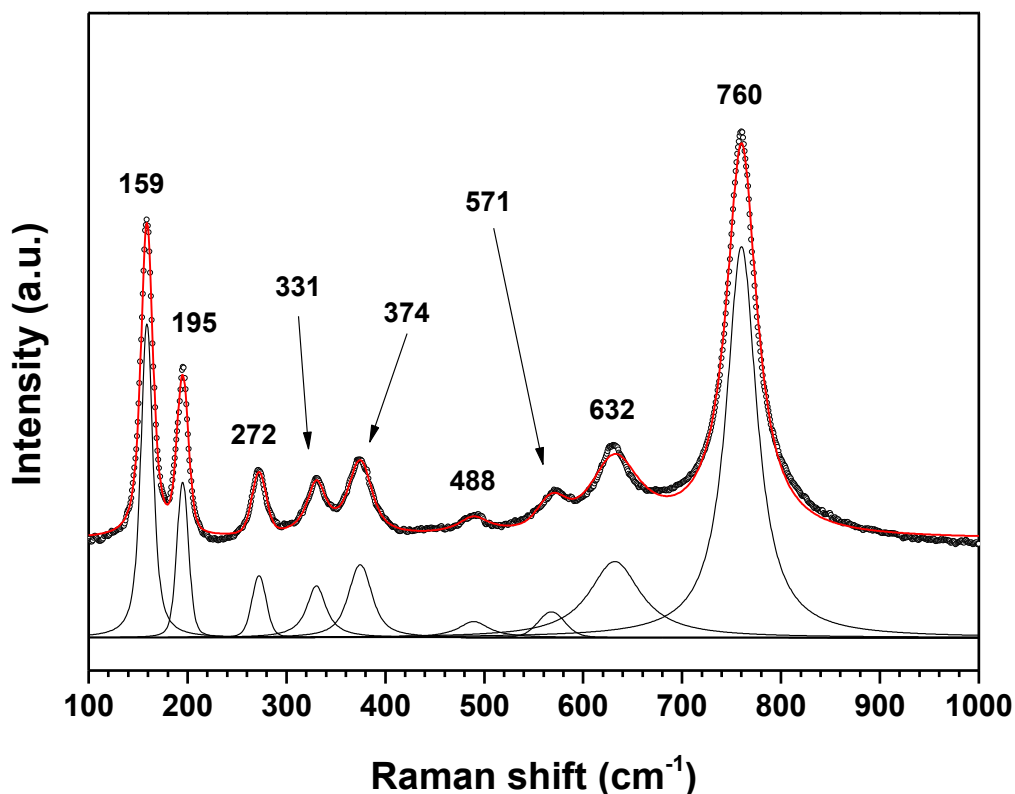


**Figure 5.** Raman spectrum of single-phase synthetic  $UTi_2O_6$  brannerite obtained by “hydroxide precipitation” (4.2), i.e. in the presence of 3 mol.% excess of titanium in the starting mixture.

## Conclusion

A new direct route was developed to synthesize pure brannerite. This protocol consisted of the precipitation of powdered hydroxide  $(An,Ti)(OH)_4 \cdot nH_2O$  precursor which was submitted to compaction into pellets and firing at 1300 °C for three days in the presence of low oxygen content (Argon atmosphere). The precipitation of the hydroxide powder allowed the preparation of highly reactive powder having a large specific surface area ( $> 100 \text{ m}^2 \cdot \text{g}^{-1}$ ) which facilitated the homogenization of the powder. This allowed the elimination of the heavy grinding step of radioactive materials. Also, the application of the hydroxide method conducted to pure powder conversely the previous protocols reported in the literature. In addition, the protocols cited in the literature involve the use of hexavalent uranium as starting reactant or of  $U_3O_8$  after grinding of  $UO_2$  in the mixture of oxides. This could induce the presence of various amounts of U(VI) within the brannerite samples, conversely to the hydroxide method which directly involved U(IV) as a reactant and thus should leave to the formation of  $U^{IV}Ti_2O_6$ . Finally, spectroscopic measurements on pure brannerite confirmed the absence of impurities such as  $TiO_2$  and  $UO_2$  in the prepared samples and confirmed the presence of tetravalent uranium only.

**Acknowledgements:** The present work was supported by the UTiLE project funded by NEEDS Ressources program (CNRS/CEA/AREVA)

## References

- [1] E. Larocque, E. Pakkala, current leaching and product recovery practice at Denison Mines Limited, *Cim Bulletin* 72(804) (1979) 172-176.
- [2] K.D. Hester, Current developments at RIO-ALGOM, ELLIOT-LAKE, *Cim Bulletin* 72(804) (1979) 181-188.
- [3] A. Wilde, A. Otto, J. Jory, C. MacRae, M. Pownceby, N. Wilson, A. Torpy, Geology and Mineralogy of Uranium Deposits from Mount Isa, Australia: Implications for Albitite Uranium Deposit Models, *Minerals* 3(3) (2013) 258-283.
- [4] M.I. Pownceby, C. Johnson, Geometallurgy of Australian uranium deposits, *Ore Geology Reviews* 56 (2014) 25-44.
- [5] R. Gilligan, A.N. Nikoloski, The extraction of uranium from brannerite – A literature review, *Minerals Engineering* 71 (2015) 34-48.
- [6] A. Eglinger, A. Tarantola, C. Durand, C. Ferraina, O. Vanderhaeghe, A.-S. André-Mayer, J.-L. Paquette, E. Deloule, Uranium mobilization by fluids associated with Ca–Na metasomatism: A P–T–t record of fluid–rock interactions during Pan-African metamorphism (Western Zambian Copperbelt), *Chemical Geology* 386 (2014) 218-237.
- [7] M.J. Lottering, L. Lorenzen, N.S. Phala, J.T. Smit, G.A.C. Schalkwyk, Mineralogy and uranium leaching response of low grade South African ores, *Minerals Engineering* 21(1) (2008) 16-22.
- [8] F.A. Charalambous, R. Ram, M.I. Pownceby, J. Tardio, S.K. Bhargava, Chemical and microstructural characterisation studies on natural and heat treated brannerite samples, *Minerals Engineering* 39 (2012) 276-288.
- [9] Y. Zhang, G.R. Lumpkin, H. Li, M.G. Blackford, M. Colella, M.L. Carter, E.R. Vance, Recrystallisation of amorphous natural brannerite through annealing: The effect of radiation damage on the chemical durability of brannerite, *Journal of Nuclear Materials* 350(3) (2006) 293-300.
- [10] S.V. Yuditsev, S.V. Stefanovsky, M.S. Nikol'skii, O.I. Stefanovskaya, B.S. Nikonov, Brannerite,  $UTi_2O_6$ : Crystal chemistry, synthesis, properties, and use for actinide waste immobilization, *Radiochemistry* 58(4) (2016) 333-348.
- [11] K.B. Helean, A. Navrotsky, G.R. Lumpkin, M. Colella, J. Lian, R.C. Ewing, B. Ebbinghaus, J.G. Catalano, Enthalpies of formation of U-, Th-, Ce-brannerite: implications for plutonium immobilization, *Journal of Nuclear Materials* 320(3) (2003) 231-244.
- [12] A.E. Ringwood, S.E. Kesson, K.D. Reeve, D.M. Levins, E.J. Ramm, in: W. Lutze, R.C. Ewing (Eds.), *Radioactive Forms for the Future* 1988, p. 233.
- [13] E.R. Vance, J.N. Watson, M.L. Carter, R.A. Day, B.D. Begg, Crystal Chemistry and Stabilization in Air of Brannerite,  $UTi_2O_6$ , *Journal of the American Ceramic Society* 84(1) (2001) 141-144.
- [14] A. Hussein, J. Tardio, S. Bhargava, Synthesis and dissolution studies of brannerite, a uranium containing mineral, CHEMECA 2008, Engineers Australia, 2008.
- [15] F.A. Charalambous, R. Ram, S. McMaster, J. Tardio, S.K. Bhargava, An investigation on the dissolution of synthetic brannerite ( $UTi_2O_6$ ), *Hydrometallurgy* 139 (2013) 1-8.
- [16] M. Colella, G.R. Lumpkin, Z. Zhang, E.C. Buck, K.L. Smith, Determination of the uranium valence state in the brannerite structure using EELS, XPS, and EDX, *Physics and Chemistry of Minerals* 32(1) (2005) 52-64.
- [17] J. Martinez, N. Clavier, A. Mesbah, F. Audubert, X.F. Le Goff, N. Vigier, N. Dacheux, An original precipitation route toward the preparation and the sintering of highly reactive uranium cerium dioxide powders, *Journal of Nuclear Materials* 462 (2015) 173-181.
- [18] C. Frontera, J. Rodriguez-Carvajal, FullProf as a new tool for flipping ratio analysis, *Physica B: Condensed Matter* 335(1-4) (2003) 219-222.
- [19] J.T. Szymanski, J.D. Scott, A crystal-structure refinement of synthetic brannerite,  $UTi_2O_6$ , and its bearing on rate of alkaline-carbonate leaching of brannerite in ore, *The Canadian Mineralogist* 20(2) (1982) 271-280.

- [20] K.S. Finnie, Z. Zhang, E.R. Vance, M.L. Carter, Examination of U valence states in the brannerite structure by near-infrared diffuse reflectance and X-ray photoelectron spectroscopies, *Journal of Nuclear Materials* 317(1) (2003) 46-53.
- [21] Y. Zhang, L. Kong, I. Karatchevtseva, D. Aughterson Robert, J. Gregg Daniel, G. Triani, Development of brannerite glass-ceramics for the immobilization of actinide-rich radioactive wastes, *Journal of the American Ceramic Society* 100(9) (2017) 4341-4351.
- [22] Y.J. Zhang, I. Karatchevtseva, M.J. Qin, S.C. Middleburgh, G.R. Lumpkin, Raman spectroscopic study of natural and synthetic brannerite, *Journal of Nuclear Materials* 437(1-3) (2013) 149-153.
- [23] L.G. Kong, D.J. Gregg, I. Karatchevtseva, Z.M. Zhang, M.G. Blackford, S.C. Middleburgh, G.R. Lumpkin, G. Triani, Novel Chemical Synthesis and Characterization of  $\text{CeTi}_2\text{O}_6$  Brannerite, *Inorganic Chemistry* 53(13) (2014) 6761-6768.
- [24] Y.J. Zhang, J. Cejka, I. Karatchevtseva, M.J. Qin, L.G. Kong, K. Short, S.C. Middleburgh, G.R. Lumpkin, Theoretical and experimental Raman spectroscopic studies of synthetic thorutite ( $\text{ThTi}_2\text{O}_6$ ), *Journal of Nuclear Materials* 446(1-3) (2014) 68-72.
- [25] E.J. Baran, C.I. Cabello, A.G. Nord, Raman-Spectra of Some M-Li- $\text{V}_2\text{O}_6$  Brannerite-Type Metavanadates, *Journal of Raman Spectroscopy* 18(6) (1987) 405-407.
- [26] R.L. Frost, B.J. Reddy, Raman spectroscopic study of the uranyl titanate mineral brannerite  $(\text{U,Ca,Y,Ce})_2(\text{Ti,Fe})_2\text{O}_6$ :effect of metamictisation, *Journal of Raman Spectroscopy* 42(4) (2011) 691-695.